Structure factors associated with the continuous melting of two-dimensional lattice gases: Models with $(\sqrt{3}\times\sqrt{3})R30°$ and $p(2\times2)$ ordered states on triangular nets

N. C. Bartelt, T. L. Einstein, and L. D. Roelofs*
Department of Physics and Astronomy, University of Maryland, College Park, Maryland 20742
(Received 16 December 1985; revised manuscript received 15 May 1986)

We study the temperature dependence of the structure factors of two lattice gases which undergo order-disorder phase transitions. Our goal is to determine how much information about the critical behavior of these phase transitions a low-energy electron-diffraction experiment *might* obtain. We use Monte Carlo simulation to compute the structure factors. Both lattice gases are on triangular nets; one has a $(\sqrt{3}\times\sqrt{3})R30°$ ordered phase; the other has a $p(2\times2)$ ordered phase. The structure factors scale almost halfway from the center of an extra spot to the zone center; for system sizes comparable to those that are physically realizable we see effective critical exponents which are typically within of order 10% of expectations based on universality. Below the transition temperature, nonlinearities in log-log plots are significant, indicating that corrections to scaling cannot be ignored. We consider how asymmetries in the structure factor reflect differences between lattice-gas systems and magnetic analogs in the same universality class and also briefly treat the effects of quenched random vacancies and of a fixed concentration of annealed vacancies.

I. INTRODUCTION

Phase transitions on the surfaces of single crystals are ubiquitous phenomena.[1] They are of interest for two reasons. The first is that through analysis of phase diagrams one hopes to understand microscopic behavior at surfaces. The second is that the understanding of the phase transitions themselves, as problems of statistical physics, is an important test of our basic understanding of two-dimensional critical phenomena. The principal tool for the investigation of surface phases is low-energy electron diffraction (LEED). In this paper we compute, using Monte Carlo simulations, the structure factor for a pair of two-dimensional phase transitions. We then analyze this data straightforwardly—as one might analyze a diffraction experiment—for critical behavior. While our discussion is couched in the language of adsorbate phase transitions, our work applies to any two-dimensional lattice gas system where the range of long-range order is limited.

Perhaps the most fundamental limitations in interpreting surface phase transitions in terms of critical phenomena are finite-size effects.[2] Terraces on surfaces limit the range of long-range order and the spatial scale of fluctuations. As single-crystal metal surfaces cannot easily be obtained with more than a hundred atomic spacings between terraces, the correlation length cannot change by much more than an order of magnitude as the surface orders. Scaling theories of second-order phase transitions predict the behavior of systems in which the correlation length becomes much greater than microscopic length scales, so it is not clear *a priori* how well they describe the behavior of typical surface systems. For example, it is difficult to know how close effective exponents measured in LEED experiments will be to exponents computed for the infinite-correlation-length limit. Our direct calculations of these effective exponents for model systems allow some expectation of their meaningfulness to be developed. Of course many of our conclusions can be inferred from the experience gained by the many Monte Carlo simulations of finite-size systems[3,4] and various exact results. Most of these works, however, are more interested in obtaining information about the infinite-system behavior than in the effective exponents themselves, and there are more efficient methods of estimating critical exponents than directly determining effective exponents. Finite-size scaling[5] and Monte Carlo renormalization[6] are examples. These methods of analysis are usually not available to the experimenter; it is difficult to change the system size or to determine many correlation functions. We also note that most of these calculations are for spin systems which have higher symmetries than the lattice gas models appropriate to surface phases,[7] as discussed in more detail below. Analyzing the structure factor also raises points not directly dealt with in most Monte Carlo work. For example, how small do wave vectors have to be before the structure factors satisfy scaling relations? There are, of course, complications other than finite-size effects in interpreting LEED experiments. Two difficulties are finite instrumental resolution[8] and multiple scattering.[9] The former limits the size of correlation lengths which can be measured. This is no difficulty if one desires information about short-range order. (LEED intensity measurements which are sensitive only to short-range correlations will have an energylike singularity at a critical point—allowing the specific-heat exponent α to be measured.[10]) In measuring long-range order one seeks the largest correlation lengths possible, requiring deconvolution of an instrumental response function from the data.[11,12] Assumptions made in the deconvolution process (for example assuming Lorentzian line shapes and circular symmetry) complicate the interpretation of the results. The ultimate resolution one can obtain by deconvolution is limited by

the accuracy with which the instrumental response can be measured. Multiple scattering, caused by strong electron-atom scattering, complicates the interpretation of the scattered intensity in terms of surface correlation functions. As the multiple scattering is short-ranged (because of the short mean free path of low-energy electrons in solids), it in principle causes no problems in the limit of large correlation lengths and small wave vectors,[13] but certainly complicates the interpretation of real experiments. For example it can break symmetries present in the kinematic structure factors by multiplying them by scattering factors dependent on both incident and final wave vectors individually (rather than on just their difference). This single-adatom effect essentially modifies the (effective) atomic form factor. Nonetheless, for extra-spot intensities, multiple scattering is expected to modify only the amplitude of corrections-to-scaling terms already present in the single scattering problem.[13] We have not included finite resolution or multiple scattering effects in our simulations.

We will study the disordering transitions of two lattice gas models which represent systems of atoms adsorbed on single crystals on a triangular array of binding sites. The first forms a $(\sqrt{3}\times\sqrt{3})R\,30°$ ordered state [Fig. 1(a)] at low temperatures. The second forms a $p(2\times2)$ structure [Fig. 1(b)]. Hereafter, we will usually refer to these lattice gas systems simply as $(\sqrt{3}\times\sqrt{3})$ and $p(2\times2)$, respectively. The studies were done at constant chemical potential fixed to yield, close to the transition temperature, coverages close to those of the perfectly ordered states. These two phases are predicted[14,15] to be able to have continuous transitions in the three- and four-state Potts model universality classes, respectively. We find, typically, sets of effective exponents which are within 10% of the Potts-model values for systems of 3888 sites.

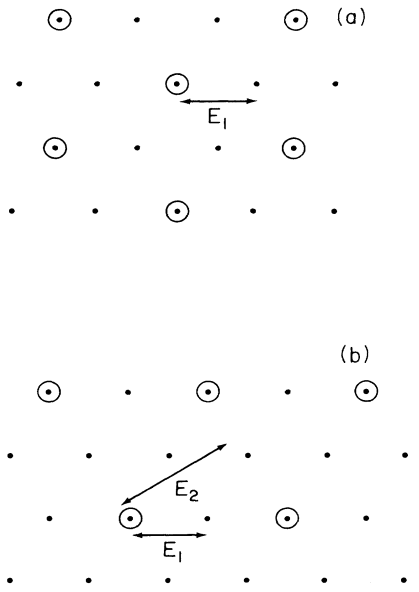

FIG. 1. Ordered states of the triangular lattice gases studied in this paper: (a) $(\sqrt{3}\times\sqrt{3})$ and (b) $p(2\times2)$. The E's indicate the (repulsive) lattice-gas energies that were used to generate these ordered states.

Another purpose of this work is to focus on the differences between the symmetries of the usually studied spin systems and these lattice gases. That these differences can be important in understanding the lattice gas phase transitions has been stressed by Huse and Fisher.[7] The differences between the spin and lattice-gas models show up as differences in the gradient terms in their Landau-Ginzburg-Wilson (LGW) Hamiltonians. The relevance of these terms has been a subject of recent discussion.[7] By studying the temperature dependence of the asymmetries in the $(\sqrt{3}\times\sqrt{3})$ structure factor we find the differences to be clearly irrelevant.

The plan of this paper is as follows. In the next section we discuss the lattice gas models in more detail. In Sec. III we present the raw data; in Sec. IV we discuss the behavior expected of the structure factors, and in Sec. V we compute the effective exponents (and amplitude ratios) which describe the data. In Sec. VI we introduce quenched and annealed defects into the lattices in the form of a fixed density of vacancies and show how they can affect the observation of the phase transition. We also show how working at fixed coverages significantly different from the saturation value of the ordered phase noticeably alters the appearance of the transition. Finally, in Sec. VII we present a summary and assessment of our findings.

II. DESCRIPTION OF THE MODELS

The lattice-gas model Hamiltonian with only pairwise interactions is

$$H=\sum_m E_m \sum_{\langle ij\rangle_m} n(\mathbf{r}_i)n(\mathbf{r}_j)\ , \tag{1}$$

where $n(\mathbf{r}_i)$ is the occupancy (0 or 1) of the lattice site at $\mathbf{r}_i$, and E_m is the energy of the mth nearest-neighbor interaction. Our simulations used the grand canonical ensemble, so the chemical potential μ controlled the coverage. To create the $(\sqrt{3}\times\sqrt{3})$ ordered state on the triangular lattice, we used nearest neighbor repulsions [E_1 in Fig. 1(a)] only. This model has been studied before in other contexts.[16] We studied the transition along the line $\mu=1.5E_1$. The coverage at the transition turned out to be approximately 0.336. The $p(2\times2)$ structure was created with nearest- and next-nearest-neighbor repulsions ($E_2=E_1/2$). The phase transition was examined along the line $\mu=1.4E_1$, which gave a critical coverage of approximately 0.248. Again similar models have been studied before.[17,18]

The structure factor is defined by

$$S(\mathbf{k},T)=\left\langle \left| \sum_j n(\mathbf{r}_j)e^{i\mathbf{k}\cdot\mathbf{r}_j} \right|^2 \right\rangle . \tag{2}$$

At wave vectors where there is long-range order, $S(\mathbf{k},T)$ is proportional to the square of the total number of atoms; elsewhere (away from T_c) $S(\mathbf{k},T)$ is simply proportional to the number of atoms.[10] The structure factor was computed using standard Monte Carlo techniques.[3,4] The boundaries of the lattices were hexagonally shaped. This

was to insure that as many of the infinite system symmetries as possible were present in the finite systems. Periodic boundary conditions were assumed. Periodic boundary conditions, of course, have no counterpart on surfaces so they are rather unrealistic, as are the boundary shapes. They minimize finite-size effects and were chosen to avoid any strongly system-dependent effects. Most of the simulations were performed on lattices with 3888 binding sites, which typify the size of defect-free regions on metal surfaces prepared using standard methods.

For each model at least 2×10^5 (and as many as 10^6) Monte Carlo steps per site were performed at each temperature. Typically the first 10^3 lattices were discarded for equilibration. Data for the structure factors were accumulated every 30 to 50 steps, which was roughly the time scale of fluctuations 10% above T_c. Along high-symmetry radial cuts (emanating from the zone center) the structure factor can be computed quickly by observing that one can sum over rows perpendicular to $\mathbf{k}$ first. Away from these high-symmetry lines, the calculation required more computer time.[19] We estimate that close to T_c, the computed structure factors are accurate to a few percent near the positions in $\mathbf{k}$ space which are coupled to the transitions; the accuracy is better further from T_c.

III. MONTE CARLO DATA

Figures 2 and 3 depict the form of the data obtained from the Monte Carlo calculations for the triangular lattice gas with the $(\sqrt{3}\times\sqrt{3})$ phase, and that with the $p(2\times2)$ phase, respectively. Figures 2(a) and 3(a) show the positions where $S(\mathbf{k})$ was computed in the surface Brillouin zone (SBZ) of the triangular lattice.

Figures 2 and 3, (b)—(e), show the structure factors 5% below T_c, close to T_c, and 5 and 10% above T_c. The data is in the form of contour plots of the logarithm of the structure factor (the horizontal axes point radially away from the zone center; that is k_a and k_r are the azimuthal and radial components of the wave vector). Finally Figs. 2(f) and 3(f) show the temperature dependence of $S(\mathbf{k})$ at the positions in the Brillouin zones associated with the superlattice order.

IV. STRUCTURE FACTOR SCALING FUNCTIONS

Figures 2 and 3 show clearly the narrowing and increase in intensity of $S(\mathbf{k})$ one expects to observe as one approaches a second-order phase transition. The phenomenological theory of second-order phase transitions predicts that the structure factor scales like[20]

$$S(\mathbf{k},T)=a_1 t^{-\gamma} X_{\pm}(a_2 t^{-\nu}\,|\,\mathbf{k}\,|\,) \tag{3}$$

for small $t\equiv|\,T-T_c\,|/T_c$ and $|\,\mathbf{k}\,|$ [where from now on we take the origin of $\mathbf{k}$ to be a position in $\mathbf{k}$ space where long-range order forms at low temperatures (i.e., $\overline{K}$ or $\overline{M}$)], $X_{\pm}(y)$ are universal functions, and a_1 and a_2 are system-dependent constants. Figure 4(a) shows some of the Monte Carlo data for $T>T_c$ for the $(\sqrt{3}\times\sqrt{3})$ system along the cut $\overline{K}\,\overline{\Gamma}$ scaled according to Eq. (3) with the three-state Potts model values of γ and ν. The critical temperature was chosen to give the best scaling. The data can be made to scale within the statistical errors of the Monte Carlo data for $\mathbf{k}$'s less than half the way to $\overline{\Gamma}$; one does not expect data far from $\overline{K}$ to scale because the lattice constant then becomes important. Data within approximately 2% of T_c cannot be made to scale, indicating the onset of finite-size effects. Multiple scattering of finite range into the substrate introduces another length scale of the order of the lattice constant,[13] and thus in an actual experiment the data might scale over a smaller (or larger) $\mathbf{k}$ region. In Fig. 4(b), the data for the $p(2\times2)$ system is scaled using four-state Potts exponents.

Because the structure factor remains finite at T_c for nonzero $\mathbf{k}$, Eq. (3) implies that the function $X_{\pm}(y)$ must vanish as $y^{-\gamma/\nu}=y^{\eta-2}$ as y gets large (that is, t small). As indicated in Fig. 5, from the slopes of plots of $\log[S(\mathbf{k})]$ versus $\log(\,|\,\mathbf{k}\,|\,)$, for the lowest temperatures in Fig. 4, we can obtain an effective exponent η. This η_{eff} depends on the range in $\mathbf{k}$ space used to determine the slope. For the lines shown in Fig. 5(a), η_{eff} varies from 0.03 to 0.17. The exact value for the three-state Potts model is $\frac{4}{15}\approx0.266$. Similarly the values of η_{eff} for the $p(2\times2)$ lattice gas, which are shown in Fig. 5(b), should be compared with the result $\eta=\frac{1}{4}$ for the four-state Potts model. For the Ising model above T_c, S is proportional to $y^{\eta-2}$ to an accuracy of 5% only when y is greater than 163,[21] while our data scales only up to y of order 10, so we do not anticipate that this is an easy way to estimate η. To obtain information about $X_{\pm}(y)$ at large y requires data not affected by the lattice size close to T_c. However, at T_c, where the correlation length is on the order of the system size, the structure factor satisfies another scaling relation:

$$S(\mathbf{k},T_c,L)=L^{\gamma/\nu}W(\mathbf{k}L)\,. \tag{4}$$

The scaling function $W(\mathbf{y})$ depends on the shape and type of boundary. It has been computed by using both conformal invariance[22] and Monte Carlo[23] for the Ising model with a variety of geometries. However, again we have $\lim_{|\,\mathbf{y}\,|\to\infty}W(\mathbf{y})\propto|\,\mathbf{y}\,|^{\eta-2}$. So even data affected by the size of the lattice can be used to obtain an estimate η_{eff} of η. Whether this estimate will be generally any better than the above one is difficult to know because of the sensitivity to the boundary. For the periodic boundaries used here, the estimates were closer to the Potts values. [Computing at the T_c reported below, we obtained plots analogous to Fig. 5, but with $\eta_{\text{eff}}\approx0.23$ and 0.30, for the $(\sqrt{3}\times\sqrt{3})$ and $p(2\times2)$, respectively. For physical boundary conditions, the η_{eff}'s might be very different.]

Figures 2 and 3 show that the structure factors are not circularly symmetric about $\mathbf{k}=0$. Equation (3) assumed that the structure factors are isotropic in the limit $T\to T_c$ and $\mathbf{k}\to0$. To attempt to understand the observed anisotropies, we first construct the power series of $S(\mathbf{k},T)$ in the deviation from the center of the extra spots. Because of the position of the peak in the structure factor for the $(\sqrt{3}\times\sqrt{3})$ system in the Brillouin zone, $S(\mathbf{k})$ must have threefold rotational symmetry. This implies that the structure factor must have the following small-$|\,\mathbf{k}\,|$ expansion:

$$S(\mathbf{k},T)=\chi(T)[1-\xi(T)^2\,|\,\mathbf{k}\,|^2 + b(T)(k_r^3+3k_a^2k_r)+\cdots]\,. \tag{5a}$$

The third term is invariant under rotations of $2\pi/3$ and even in k_a: $\mathrm{Re}[(k_r+ik_a)^3]=k_r-3k_a^2k_r$. Similarly the small-$|\mathbf{k}|$ expansion for the $p(2\times2)$ lattice gas is

$$S(\mathbf{k},T)=\chi(T)[1-\xi(T)^2|\mathbf{k}|^2 +b(T)(k_a^2-k_r^2)+\cdots]\,. \quad (5b)$$

The structure factors for the Potts models on square lattice, however, have no anisotropic (non-$|\mathbf{k}|^2$) terms until fourth order in k_a and k_r. On triangular and honeycomb lattices, the leading anisotropic term is of sixth order in k_a and k_r.

In real systems the adsorbed atoms might not sit on a

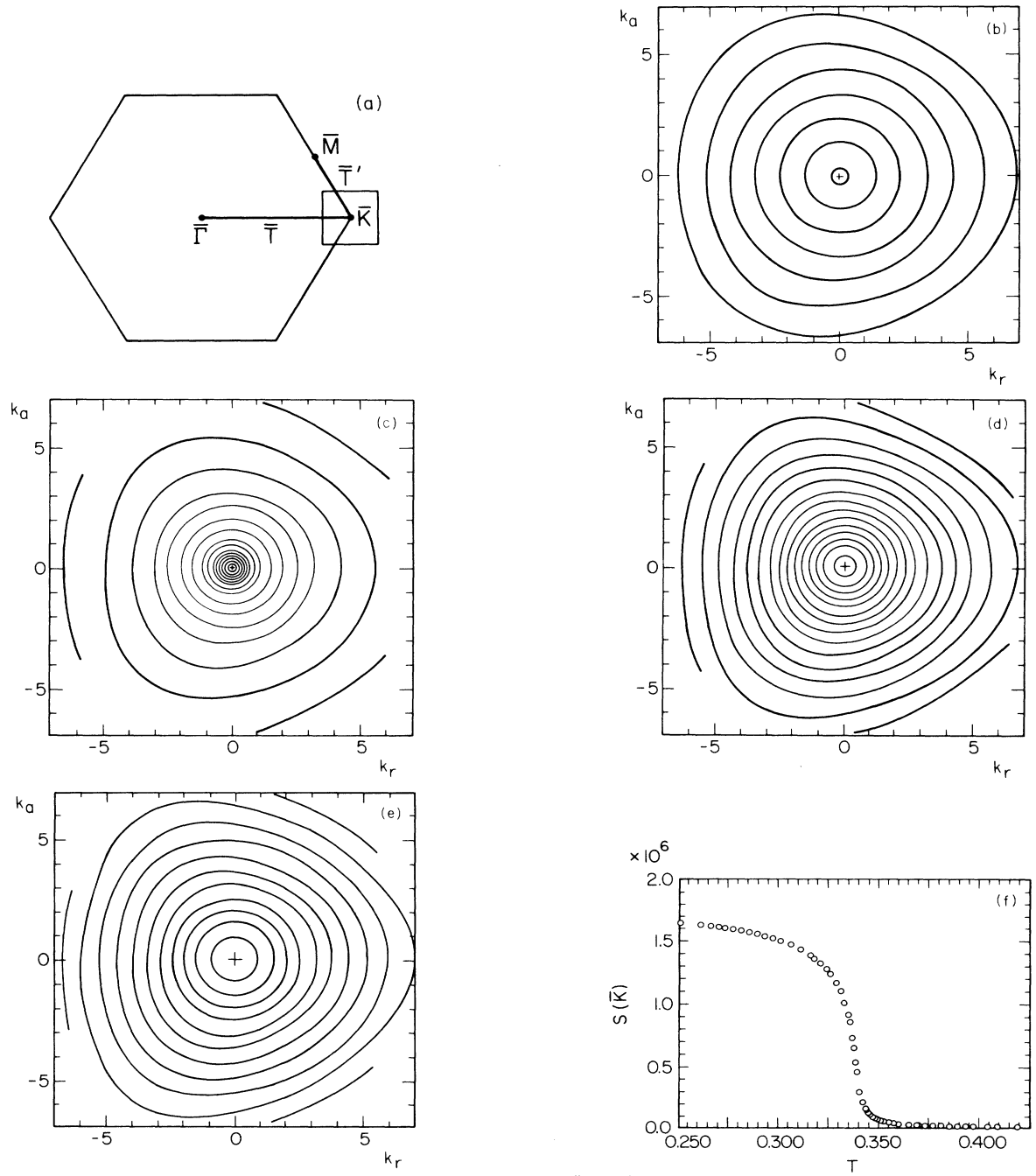

FIG. 2. Monte Carlo data for the triangular lattice gas with the $(\sqrt{3}\times\sqrt{3})$ ordered state. The surface Brillouin zone (SBZ) and the regions where the structure factor were computed (along cuts $\overline{K\Gamma}$ and $\overline{KM}$, and within the square) are shown in (a). Contour plots of the structure factor within the square of (a) are shown in (b)–(e): (b) $T=0.325E_1$ ($\approx5\%$ below T_c); (c) $T=0.338E_1$ (approximately T_c); (d) $T=0.355E_1$ ($\approx5\%$ above T_c); and (e) $T=0.382E_1$ ($\approx10\%$ above T_c). Contour increments are on a (common) logarithmic scale separated by 0.1 except for (c) where the increment is 0.2. For (b) the outermost contour level is 2.6, for (c) it is 3.0, and for (d) and (e) it is 3.2. (f) The temperature dependence of $S(\bar{K})$.

discrete lattice of sites—e.g., in a physisorbed system they easily fluctuate from their preferred positions. This violation of the lattice gas symmetries can lead to additional terms in the above expansions.[24]

In each case we seek the temperature dependence of the anisotropy coefficient b. There are at least three possibilities. The first is that the scaling functions of Eq. (3) are anisotropic: that is, they depend on $\mathbf{k}$ rather than just $|\mathbf{k}|$. Then $b(T)$ in Eq. (5a) would be proportional to ξ^3 or $t^{-3\nu}$, and $b(T)$ in Eq. (5b) would be proportional to $t^{-2\nu}$. As the scaled structure factors are predicted to be universal and the scaled structure factors of the Potts models are isotropic, observation of this type of behavior would mean that the lattice gas is in a non-Potts model

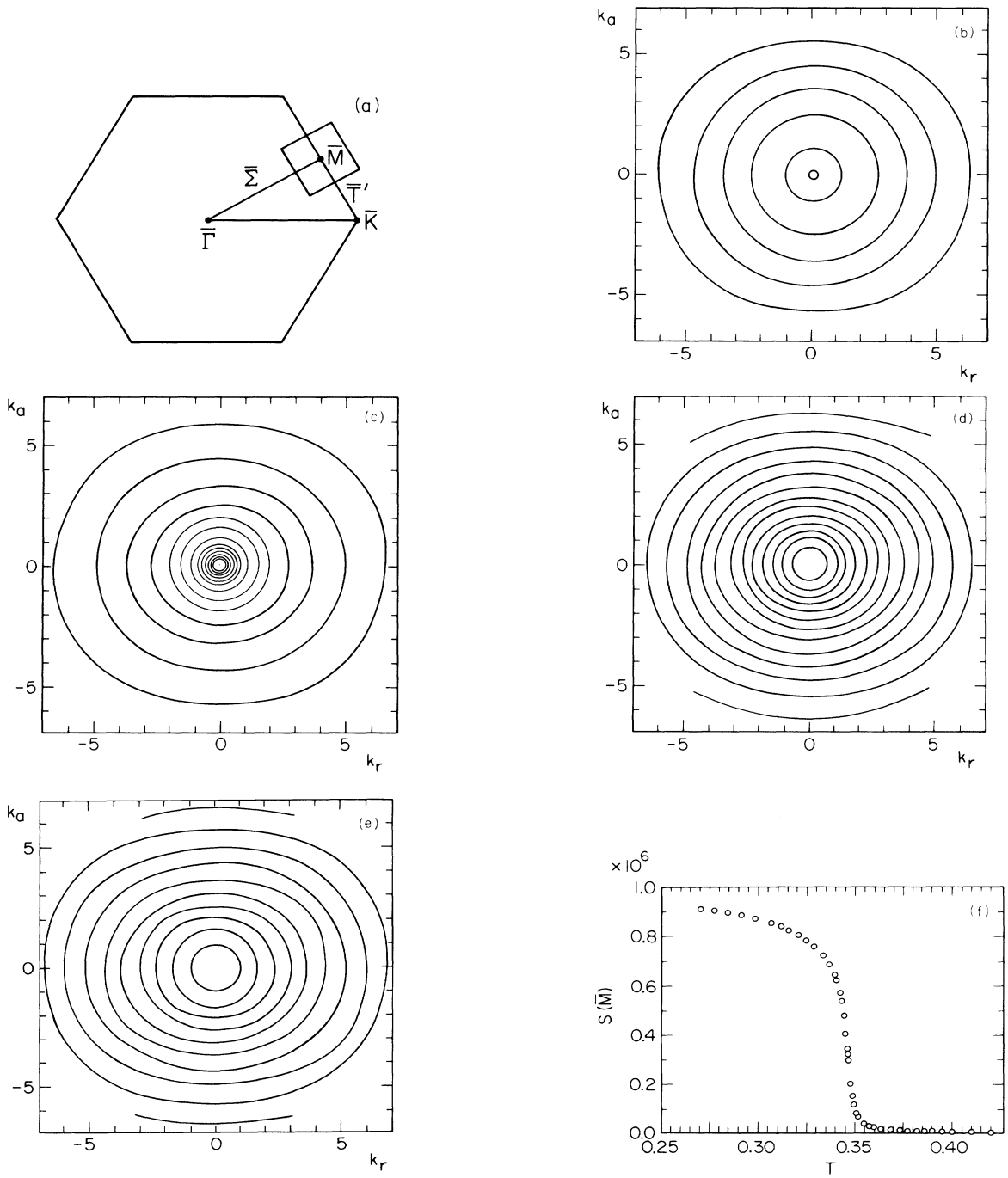

FIG. 3. Similar to Fig. 2 but for the $p(2\times2)$ ordered state. (a) SBZ. The contour plots for (b) $T=0.323E_1$ (the outermost contour is 2.4); (c) $T=0.344E_1$ (the outermost contour is 2.8); (d) $T=0.363E_1$ (the outermost contour is 3.0); and (e) $T=0.382E_1$ (the outermost contour is 3.0). (f) Temperature dependence of $S(\bar{M})$. The contour increments are the same as in Fig. 2.

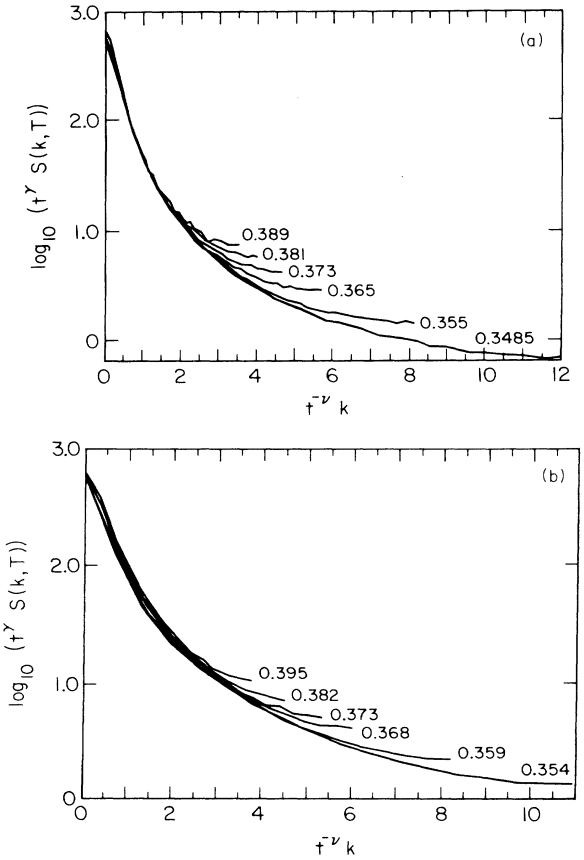

FIG. 4. Structure factor above T_c scaled according to Eq. (3) for (a) the $(\sqrt{3}\times\sqrt{3})$ lattice gas, assuming γ and ν of the three-state Potts model and $T_c=0.338E_1$ (**k** along $\overline{T}$, with the origin at $\overline{K}$) and for (b) the $p(2\times2)$ triangular lattice gas, assuming four-state Potts model exponents and $T_c=0.345E_1$ (**k** along $\overline{\Sigma}$, with the origin at $\overline{M}$).

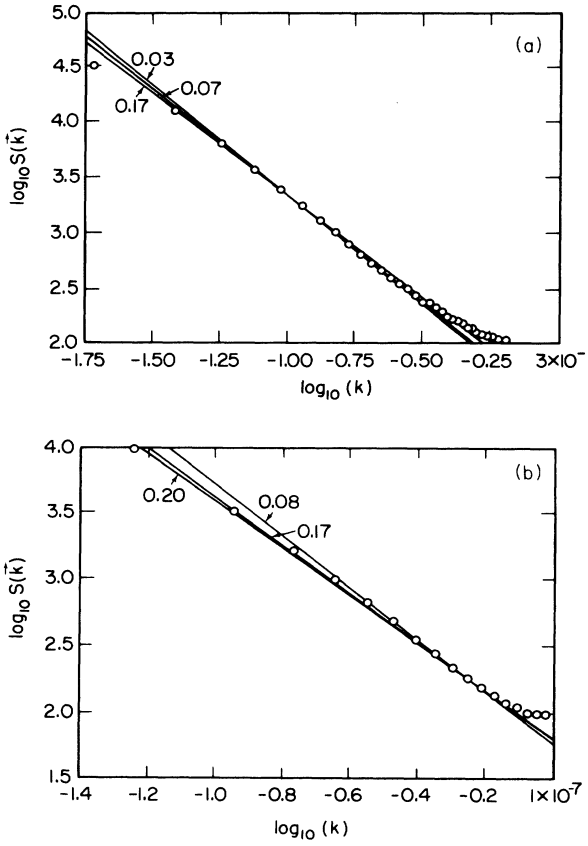

FIG. 5. Log-log plots of the **k** dependence of the structure factors for (a) the $(\sqrt{3}\times\sqrt{3})$ lattice gas (**k** along $\overline{T}$ from $\overline{K}$) and (b) the $p(2\times2)$ lattice gas (**k** along $\overline{\Sigma}$ from $\overline{M}$). In each case the temperature is the lowest of those appearing in Fig. 4. The slopes of the lines are $-(2-\eta_{\text{eff}})$, and each is labeled by the resulting estimate η_{eff}, showing the dependence on the fitted **k** range.

universality class, and thus the predictions of the standard Landau-Ginzburg-Wilson classification scheme would be incorrect.

The second possibility is that the scaled structure factors are isotropic and the anisotropy is a correction to scaling,[25]

$$S(\mathbf{k},T)=t^{-\gamma}[X_{\pm}(|\mathbf{k}|t^{-\nu})+gt^{\Delta}Y_{\pm}(\mathbf{k}t^{-\nu})]\ , \tag{6}$$

where Δ is the correction to scaling exponent and $Y_{\pm}(\mathbf{y})$ are (universal) corrections to scaling functions. For the $(\sqrt{3}\times\sqrt{3})$ lattice gas $Y_{\pm}(\mathbf{y})$ would have the following small y expansions

$$\lim_{y\to0} Y_{\pm}(\mathbf{y})=c_1^{\pm}|\mathbf{y}|^2+c_2^{\pm}(y_r^3-3y_a^2y_r)\ . \tag{7}$$

Thus the form of Eq. (5a) is reproduced with $b(T)/\xi^3\propto t^{\Delta}$.

A third possibility for the cause of the asymmetry is a nonlinear scaling field: one must distinguish the $|\mathbf{k}|$ of Eq. (2) (shifted by the **k** of the ordered state) from that of Eq. (3), which we will denote k_s. For example, for the $(\sqrt{3}\times\sqrt{3})$ case we expect that

$$k_s^2=|\mathbf{k}|^2+d_1(k_r^3-3k_a^2k_r)+d_2t|\mathbf{k}|^2+\cdots\ . \tag{8}$$

That is, in the wave-vector scaling field one must consider the terms nonlinear in $|\mathbf{k}|^2$ which are allowed by symmetry. This effect would also induce the behavior described by Eq. (5), with $b(T)/\xi^3\propto t^{5/6}$: placing the scaling field defined by Eq. (8) in the scaling function of Eq. (3) and expanding in small $t^{-\nu}k_s$ yields

$$S(\mathbf{k},T)=a_1t^{-\gamma}\{X_{\pm}(0)+(a_2^2/2)t^{-2\nu}[|\mathbf{k}|^2+d_1(k_r^3-3k_a^2k_r)]X_{\pm}''(0)+\cdots\}\ . \tag{9}$$

Comparison with Eq. (6) then implies $\Delta=\nu=\frac{5}{6}$.

We now discuss predictions of the behavior of $b(T)$ for the $(\sqrt{3}\times\sqrt{3})$ case. We can imagine fields applied to these systems which distinguish the lattice gas system from the more symmetric counterpart. The appropriate field, called triaxial chiral, can be written as a term in its LGW Hamiltonian:

$$H_3=g_3\mathrm{Im}\left[\int d^2r\psi\nabla_1\nabla_2\nabla_3\psi^*\right], \tag{10}$$

where $\psi(\mathbf{r})$ is the (coarse-grained) order-parameter density and ∇_1, ∇_2, and ∇_3 are gradient operators in the directions of three principal axes. This term produces a difference in domain wall energies if the two abutting states are exchanged.[7] The expectation value of this term is

$$\langle H_3\rangle\propto g_3\int d^2k(k_r^3-3k_a^2k_r)\mathscr{S}(\mathbf{k},T), \tag{11}$$

with $\mathscr{S}(\mathbf{k},T)=\langle\psi_{\mathbf{k}}\psi_{\mathbf{k}}^*\rangle$ and $\psi_{\mathbf{k}}\propto\int d^2r\psi e^{i\mathbf{k}\cdot\mathbf{r}}$. As $S(\mathbf{k},T)$ is proportional to $\mathscr{S}(\mathbf{k},T)$ for sufficiently small $|\mathbf{k}|$, $b(T)$ in Eq. (5a) is also nonzero if g_3 is nonzero. Huse and Fisher[7] predict that this term is an irrelevant perturbation of the three-state Potts model; hence for sufficiently small g_3, the anisotropy in the structure factor should be governed by Eq. (6). Den Nijs computes $\Delta=\frac{5}{6}$.[26] (This exponent is consistent with one which is allowed by conformal invariance.[27])

For the $p(2\times2)$ triangular case, the lowest-order term distinguishing it from the four-state Potts LGW Hamiltonian is a nonisotropic (sixfold symmetric) quadratic term:

$$H_6=g_6\sum_j(\mathbf{G}_j\cdot\nabla\phi_j)^2, \tag{12}$$

where the $\phi_j(\mathbf{r})$ are the three components of the order parameter field, and the $\mathbf{G}_j$ are the three "primitive" reciprocal lattice vectors of the $p(2\times2)$ ordered state. This term breaks the degeneracy of wall energies between unlike domains, but is not chiral-like. While this term, which leads to the anisotropy terms in Eq. (5b), is omitted in standard LGW classifications,[16,18] we will see that it is not obviously negligible.

V. EXPONENT ANALYSIS AND DISCUSSION

In this section we compute $\chi(T)$, $\xi(T)$, and $b(T)$ using the Monte Carlo data, and analyze the results by computing effective exponents. We begin by defining and discussing these effective exponents. From the data we computed the temperature dependence of the correlation length, susceptibility and order parameter. Near T_c the temperature dependence of one of these quantities $G(T)$ is expected to be given by

$$G(T)=G_0t^{-\lambda}(1+a_G^{\pm}t^{\Delta}+\cdots). \tag{13}$$

The expression in parentheses represents the correction to scaling factor to the asymptotic power law with exponent λ. Because of these corrections we expect to observe an effective exponent[28]

$$\lambda_{\mathrm{eff}}=-\frac{\partial\ln G}{\partial\ln t^*}, \tag{14}$$

where t^* is an estimate of t—typically one does not know T_c beforehand, making the estimate necessary. If T_c is available (for example from a low-resolution measurement on a relatively defect-free surface[10]) then the convergence of λ to λ_{eff} is described by

$$\lambda_{\mathrm{eff}}=\lambda-a_G^{\pm}\bar{t}^{\Delta}\Delta+\cdots, \tag{15}$$

where $\bar{t}$ is a suitable average over the range of measurement. If one does not know T_c, then

$$\lambda_{\mathrm{eff}}=\frac{(T-T_c^*)}{(T-T_c)}(\lambda-a_G^{\pm}\bar{t}^{\Delta}\Delta+\cdots). \tag{16}$$

One procedure for constructing the estimate of T_c, T_c^*, is to maximize the linearity of the log-log plots, that is, choosing T_c^* by requiring

$$\frac{\partial^2\ln G}{\partial(\ln t^*)^2}=0. \tag{17}$$

This yields

$$T_c^*=T_c\left[1+\frac{a_G^{\pm}\Delta^2}{\lambda}\bar{t}^{\Delta+1}+\cdots\right], \tag{18a}$$

and

$$\lambda_{\mathrm{eff}}=\lambda-a_G^{\pm}\Delta(1+\Delta)\bar{t}^{\Delta}. \tag{18b}$$

Thus the convergence of T_c^* to T_c is faster than the convergence of the effective exponents, and the lack of knowledge of T_c only affects the amplitude of convergence of the effective exponent, not the power. This procedure of estimating T_c will be used in what follows. Notice one always expects a term with $\Delta=1$ because of the possibility of terms quadratic in $(T-T_c)$ in the definition of t in Eq. (13).

For the one or two decades of reduced temperature which we analyze there is little sense of the convergence described by Eq. (18). All we can do is quote the effective exponents. We will also see that determining the thermal range over which to apply the above method requires some thought.

Given the structure factor, we need to define the correlation length ξ, which is some measure of the inverse width of the structure factor, and the susceptibility χ, which is some measure of its height. These definitions are not unique.[29] The definitions of ξ and χ which we use are the parameters of the Lorentzian which best fit the structure factor. Explicitly we find the ξ and χ which minimize the function

$$R(\xi,\chi)=\sum_i\left[S(\mathbf{k}_i,T)-\frac{\chi}{1+\xi^2|\mathbf{k}_i|^2}\right]^2. \tag{19}$$

These definitions differ slightly from those given by Eq. (5). Assuming that $S(\mathbf{k},T)$ has the scaling form of Eq. (3), it is easy to show that ξ and χ defined in this way are independent of the large $|\mathbf{k}|$ cutoff sufficiently close to T_c and that $\xi\propto t^{-\nu}$ and $\chi\propto t^{-\gamma}$ (with nonuniversal proportionality constants). For finite systems without periodic boundary conditions, the δ functions in S due to long-range order beneath T_c will be approximated by functions of width proportional to $1/L$. To avoid these

effects one must not consider data close to $\mathbf{k}=0$. For our systems, which have periodic boundary conditions, the structure factor is only nonzero on a finite grid of points with spacing on the order of $1/L$, so this causes no complications: avoiding the δ functions means omitting the point at $\mathbf{k}=0$. Figure 6 shows the temperature dependence of ξ for the $(\sqrt{3}\times\sqrt{3})$ lattice gas computed using cut $\overline{K\Gamma}$. The correlation length gets large near the transition. For this figure the data at $\mathbf{k}=0$ were not used in the fit at all temperatures. In later analyses, once T_c was estimated, we included $\mathbf{k}=0$ above T_c, decreasing the noise in ξ. As an example of the results from a different and dangerous (although tempting) definition of ξ, we obtained the correlation length from a linear least squares fit of $S^{-1}(\mathbf{k})$ versus $|\mathbf{k}|^2$ using data $\frac{1}{4}$ of the way to the zone center. In this fitting procedure data away from $\mathbf{k}=0$ is weighted so heavily that sufficiently close to T_c it will be insensitive to data in the scaling limit of Eq. (3). Thus this correlation length will have an energylike singularity[10] rather than a divergence (although one might not see the energylike singularity until one is very close to T_c because this effect depends on a nonzero η). Figure 6 compares this correlation length to the one obtained from Eq. (19).

Figure 7 shows the temperature dependence of the estimate of χ obtained from Eq. (19) not using data at $\mathbf{k}=0$. Beneath T_c, where there is a spontaneous magnetization $M(T)$, $S(0,T)$ for a finite system sufficiently far from T_c can be approximated by

$$S(0,T)=L^4[M^2(T)+L^{-2}\lim_{\mathbf{k}\to 0}S(\mathbf{k},T)]\ , \tag{20}$$

where L is the linear dimension of our lattices, or the size of defect-free regions in experiment. We will approximate the limit in Eq. (20) by $\chi(T)$ defined by Eq. (19). Because of the small deviations of the structure factors from Lorentzians, the error we make in this approximation is negligible. Figure 7 show the temperature dependence of $M^2(T)$, computed using Eq. (20), for the $(\sqrt{3}\times\sqrt{3})$ lattice gas. This can be compared with $S(0,T)$ in Fig. 2(f). Far from T_c, when $\chi(T)$ is small, it is unnecessary to take it into account when computing $M^2(T)$ because of the L^{-2} factor in Eq. (20). Thus it is not always necessary to deconvolute an instrument response function from the data to obtain $M^2(T)$.

The first step in the effective exponent analysis was to decide how much of the data should be accounted for by the form of Eq. (13). Near T_c, when the correlation length becomes on the order of the system size, Eq. (13) breaks down; we decided to consider only data where the correlation length was less than half the maximal correlation length. We emphasize that this criterion can be applied in analysis of experimental data. So, from Fig. 6, we only used data with T greater than $0.348E_1$ or T less than $0.334E_1$ for the $(\sqrt{3}\times\sqrt{3})$ lattice gas. A test of this criterion is that the results should not be sensitive to it; if one analyzes too close to T_c the effective exponents will start to decrease. (Of course, it might be difficult to distinguish this decrease initially from one caused by corrections to scaling.) An alternative procedure would be to analyze data that evidently scales.[30] The danger of this method is that one might choose T_c so that data close to T_c scales when it really should not. One is particularly prone to such a poor choice when the thermal range of the data is small. How large the correlation length is compared with the system size when finite-size effects become important is, of course, system dependent. (It depends on boundary conditions, for example.) For the systems studied here, the half-maximal-correlation-length criterion seems safe, as will be shown later. For systems with boundary conditions other than periodic—surface systems, for example—the maximal correlation length is less,[22] so that if one used this criterion one would analyze data further from T_c. We do not know at what (small) length scales corrections to scaling become important far from T_c; our *effective* exponents are defined over data as far as 25% away from T_c. Just as it is important to determine the temperature region where finite-size effects become important, it is desirable to locate the temperature range where corrections to scaling become evident; data far from T_c should not simply be discarded.

For χ and ξ above T_c we chose the thermal scaling

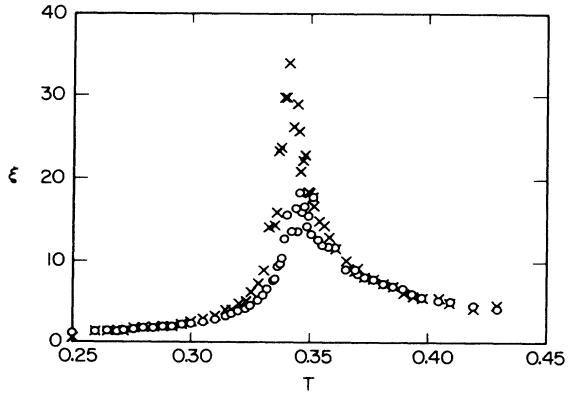

FIG. 6. Temperature dependence of the correlation length for the $(\sqrt{3}\times\sqrt{3})$ lattice gas for cut $\overline{T}$ (from $\overline{K}$ toward $\overline{\Gamma}$); $\times$'s come from a fit weighting the points near $\overline{K}$ more heavily than the fit used to generate the $\circ$'s, as described in the text.

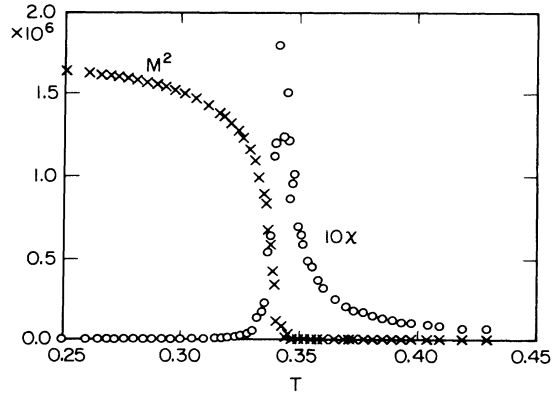

FIG. 7. Temperature dependence of χ ($\circ$), and M^2 ($\times$) for the $(\sqrt{3}\times\sqrt{3})$ lattice gas. Note the large critical amplitude ratio of χ above and beneath T_c; deducing exponents for critical scattering below T_c is difficult experimentally.

field [t in Eq. (14)] as $|1-T_c/T|$, following not uncommon practice,[31,32] rather than $|1-T/T_c|$, because this choice reproduces the result that χ and ξ approach zero rather than a constant as T goes to infinity. We thus expect corrections to scaling caused by nonlinear terms in the scaling field to be less—the two definitions of t differ by terms of order t^2. Using $t=|1-T/T_c|$ turns out to make differences on the order of the statistical errors quoted below.

Figures 8(a) and 9(a) show the results of the fits of χ to $t^{-\gamma}$ and ξ (from cut $\bar{K}\bar{\Gamma}$) to $t^{-\nu}$ above T_c. The fit of χ was used to estimate T_c because the uncertainties in determining χ were less than determining ξ. Using ξ gave results consistent with using χ, but with larger statistical error. The χ^2 of the resulting fits were consistent with estimates of the statistical error; there is no evidence for corrections to scaling. (N.B. By the χ^2 of a least-squares fit we mean the sum of the squares of the deviations of the data from the fitting function, not the square of the susceptibility.) We estimate $\gamma_{\text{eff}}=1.25\pm0.07$, $\nu_{\text{eff}}=0.77\pm0.05$, and $T_c^*=0.338\pm0.002E_1$. The error estimates are our estimates of the uncertainties caused by statistics *only* and not by systematic effects such as corrections to scaling or finite-size effects. To estimate the uncertainties we used the standard formula for error propagation:[33]

$$\sigma_f^2=\sum_i\left[\frac{\partial f}{\partial y_i}\right]^2\sigma_i^2\,, \tag{21}$$

where f is a quantity we are estimating (an effective exponent, for example), y_i are our data points from the Monte Carlo simulations, and (σ_i) and σ_f are the standard deviations of the probability distributions for the data and f, respectively. That is, to determine the uncertainty in f we computed how much f changed when we varied each data point. The above quoted uncertainties came from uncertainties in the structure factors varying from 2 to 5%, depending on T and $\mathbf{k}$.[34] For the three-state Potts model,[35] $\gamma=\frac{13}{9}\approx1.44$ and $\nu=\frac{5}{6}\approx0.83$. The effective T_c compares well with the estimate of $0.335E_1$ from finite-size (transfer matrix) scaling (using semi-infinite strips of width six and nine lattice sites), the estimate of $0.3395\pm0.0005E_1$ from analysis of block distribution functions (in a procedure similar to Binder's[36]), and the estimate of $0.338\pm0.002E_1$ from analysis of integrated structure factors.[10] There is no reason for these numbers to agree exactly—they all should lie in the finite-size rounded region, however. Figure 9(b) shows the log-log plot for ξ derived from cut $\bar{K}\bar{M}$ rather than $\bar{K}\bar{\Gamma}$. Comparison with Fig. 9(a) shows a negligible difference in effective exponents.

Given the thermal fitting range $0.348E_1<T<0.410E_1$, γ_{eff} and ν_{eff} are indeed *effective* exponents. Changing the lower cutoff to $0.345E_1$ or to $0.358E_1$, that is changing it from 3% to 2% or to 6% above T_c, did not move the effective exponents outside the statistical uncertainties, leading us to believe that the quoted effective exponents are independent of finite-size effects. Because of the lack of evident corrections to scaling, decreasing the upper cutoff of the thermal fitting range simply increases the statistical error in the estimates of the effective exponents.

Figures 8(b) and 8(c) show the effective exponent γ when T_c is fixed at $0.334E_1$ and $0.340E_1$—well outside our statistical estimate of T_c. The deviations from linearity in these log-log plots, although statistically significant, are not large; one can easily believe the deviations could be accounted for by corrections to scaling. Indeed, fitting to the form of Eq. (13) including corrections to scaling yields a χ^2 which is of the order of the χ^2 in the fit in Fig.

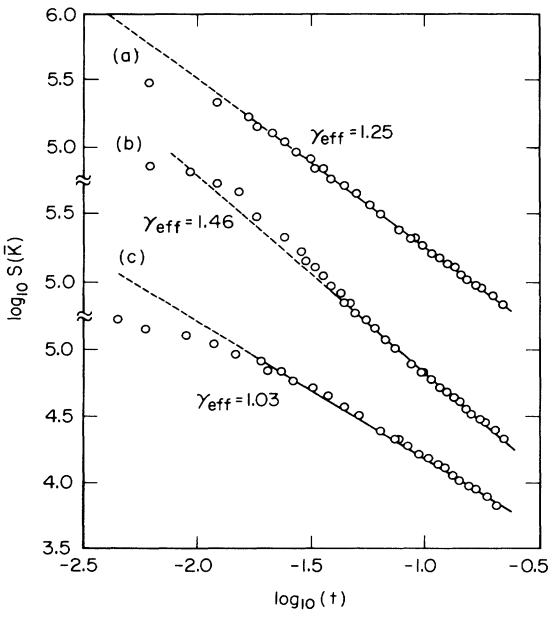

FIG. 8. Log-log plots of χ above T_c for the $(\sqrt{3}\times\sqrt{3})$ lattice gas with three estimates of T_c: (a) $T_c=0.338E_1$ (the best fit), (b) $T_c=0.334E_1$, and (c) $T_c=0.342E_1$. The effective exponents come from least-squares fits of the data over the range indicated by the solid line and suggest their sensitivity to T_c.

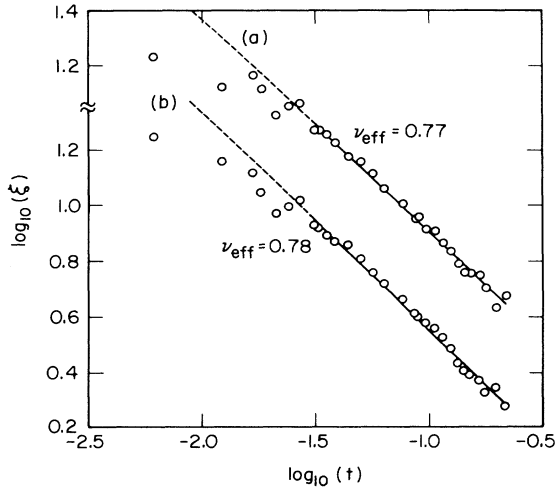

FIG. 9. Log-log plots of the correlation length ξ above T_c for the $(\sqrt{3}\times\sqrt{3})$ lattice gas derived from (a) cut $\bar{T}$, and (b) cut $\bar{T}'$, indicating the isotropy of the exponent.

8(a). This perhaps gives some feel for the systematic errors possible in fitting over such a small reduced temperature range.

Below T_c, the situation is different. Figure 10(a) shows $\log(M^2)$ versus $\log(t)$ for $T_c^*=0.338E_1$. Nonlinearities are clearly present. In fact there is no choice of T_c which makes the data linear over the entire fitting range. Evidently corrections to scaling are larger below than above T_c. As the ratios of amplitudes of corrections to scaling are expected to be universal, this problem can be expected to be a general characteristic of these types of transitions.

As $T\rightarrow T_c$, the ratio of ξ, and of χ, above and beneath T_c is universal. For the Ising model the ratio of correlation lengths defined by Eq. (5),[37] above and below T_c, is approximately 3.16 and the ratio of susceptibilities is approximately 38.[38] For this lattice gas, with the ξ and χ defined by Eq. (19), we observe ratios of 3.2 ± 0.6 and 43 ± 12, respectively.[39] Because of the evident corrections to scaling beneath T_c, the *systematic* errors in these numbers could be quite large. (When we only analyze data up to half the maximum values of t in the above analysis, we obtain 3.1 ± 0.7 and 32 ± 12 for the correlation length and susceptibility ratios.) For similar calculations of the three-state Potts model[40] on a 36×36 square lattice we find 4.1 ± 0.2 and 43 ± 3 for $0.015<t<0.1$. The large ratio for χ means that χ will be experimentally much more difficult to measure beneath T_c. Further confounding attempts to determine γ' and ν' is the need to deconvolute the instrument response function in order to separate the δ function from the k-dependent scattering.

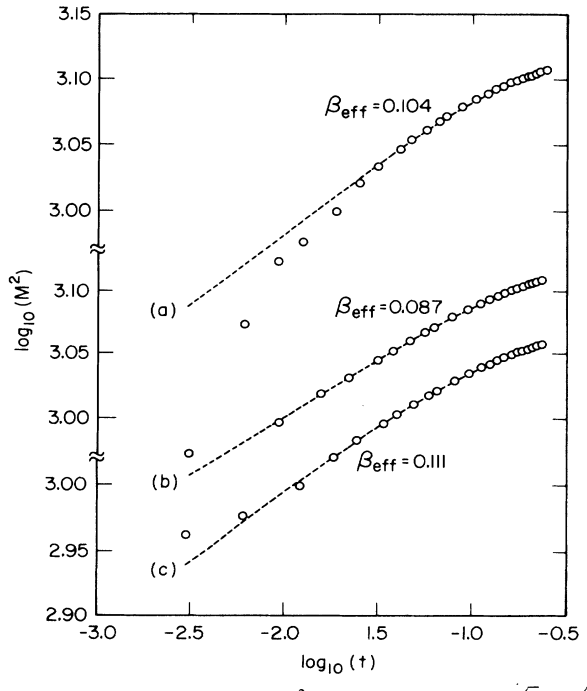

FIG. 10. Log-log plots of M^2 below T_c for the $(\sqrt{3}\times\sqrt{3})$ lattice gas with (a) $T_c=0.338E_1$, (b) $T_c=0.335E_1$, and (c) $T=0.336E_1$. The fits for (a) and (b) include a nonlinear term in the thermal fitting fitting; (c) includes a correction to scaling with $\Delta=\frac{2}{3}$.

One strategy to minimize the effects of corrections to scaling would be to limit the thermal fitting range to small t. In general there is not sufficient data to make this tactic feasible. Moreover, in some cases we have some idea of the form of the leading corrections to scaling, and so we take them into account. One source of corrections to scaling is a nonlinear term in t in the scaling field. Figure 10(a) shows the resulting $\beta_{\rm eff}$ from a fit of M to $(|t|+bt^2)^{2\beta}$. Clearly this type of correction to scaling can account for the nonlinearities in the log-log plots. We next allowed T_c^* to vary from the value determined from the data above T_c. Choosing T_c to minimize the χ^2 of the fit to M yields $\beta_{\rm eff}=0.087\pm0.010$, $\gamma'_{\rm eff}=1.41\pm0.14$, $\nu'_{\rm eff}=0.59\pm0.07$, and $T_c=0.335\pm0.002E_1$. (For the three-state Potts model, $\beta=\frac{1}{9}\approx0.111$, while $\gamma'=\gamma=\frac{13}{9}\approx1.44$ and $\nu'=\nu=\frac{5}{6}\approx0.83$.) Again the quoted uncertainties are estimates of the statistical uncertainty only. Figure 10(b) shows the log-log plots for $\beta_{\rm eff}$. For comparison, choosing T_c to maximize the linearity of the log-log plot assuming no corrections to scaling yields $T_c^*=0.334\pm0.002E_1$ and $\beta_{\rm eff}=0.073\pm0.010$. Notice that this T_c is significantly lower than those obtained from the data above T_c, while a consistent T_c is obtained when corrections are included. Another source of corrections to scaling is irrelevant scaling fields. One would like to fit to the form $M^2\propto t^{2\beta}(1+bt^{\Delta})$. Unfortunately there is not sufficient data to justify two more parameters in the fit. Nienhuis has predicted[41] that the smallest Δ for the three-state Potts model is $\frac{2}{3}$. Fixing $\Delta=\frac{2}{3}$ yields the fits shown in Figs. 10(c) and 11. We estimate $\beta_{\rm eff}=0.111\pm0.019$, $\gamma'_{\rm eff}=1.39\pm0.16$, $\nu'_{\rm eff}=0.60\pm0.07$, and $T_c^*=0.336\pm0.002E_1$. Although one cannot determine the form of the corrections to scaling from the data, one can still profitably quote effective exponents assuming

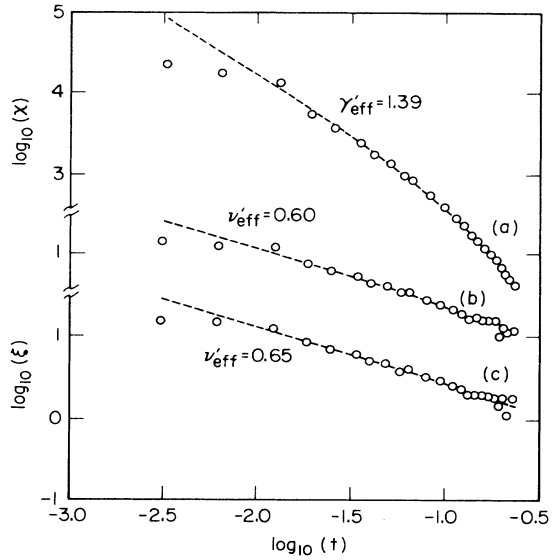

FIG. 11. Log-log plots for the $(\sqrt{3}\times\sqrt{3})$ lattice gas below T_c for (a) χ, (b) ξ derived from cut $\overline{T}$, and (c) ξ derived from cut $\overline{T}'$. T_c was chosen to be $0.336E_1$. The fits assume a correction to scaling with $\Delta=\frac{2}{3}$.

their form: including the expected corrections to the three-state Potts model yields effective exponents closer to the three-state Potts values. The exponent $\nu'_{\rm eff}$ is an exception; not including corrections to scaling gives $\nu'_{\rm eff}=0.72\pm0.08$ (using $T_c=0.336E_1$). However, the statistical errors in ξ at large t, which are not present in M^2 and χ (see Fig. 11), give us less confidence in the fits with corrections included—the correction to scaling tries to accommodate the statistical fluctuations.

Figure 12 shows the result of a fit which allowed nonzero $b(T)$ in Eq. (5a); $\log(b/\xi^3)$ is plotted as a function of $\log(t)$. As discussed in Sec. IV, Eq. (6) suggests that the effective exponent might be a correction-to-scaling exponent, $\Delta_{\rm eff}$, governing the effect of the field which causes the threefold anisotropy. We conclude $\Delta_{\rm eff}=0.83\pm0.20$, compared to den Nijs's prediction[26] that the triaxial chiral field, i.e., Eq. (10), has $\Delta=\frac{5}{6}$. If nothing else, the data suggest that the triaxial chiral field is indeed irrelevant.

The same analysis was then used on the $p(2\times2)$ lattice gas. It is expected to be in the universality class of the four-state Potts model[35] ($\gamma=\gamma'=\frac{7}{6}\approx1.17$, $\nu=\nu'=\frac{2}{3}\approx0.67$, $\beta=\frac{1}{12}\approx0.083$). For this system, data with T less than $0.336E_1$ or greater than $0.354E_1$ were used in the fits for the effective exponents. This range was determined with the half-maximal correlation length criterion. Minimizing the χ^2 of the fit for $\gamma_{\rm eff}$ yields $T_c^*=0.344\pm0.002E_1$, $\gamma_{\rm eff}=1.13\pm0.06$, and $\nu_{\rm eff}=0.70\pm0.09$ (Fig. 13). Again there is no statistical evidence for corrections to scaling. The value of T_c^* is consistent with the result $0.345\pm0.001E_1$ from a block distribution analysis.[36] Here the lower thermal cutoff could not be decreased without significantly lowering the effective exponents. Figure 14 shows the log-log plot of M^2 with $T_c^*=0.344E_1$. Nonlinearities are again present which cannot be completely removed by changing T_c. We find that the ratios of correlation length and susceptibility above and below T_c are 3.9 ± 0.7 and 43 ± 12, respectively. (Analyzing only the half of the data closest to T_c yields 3.9 ± 0.9 and 35 ± 15.) For the four-state Potts models similar simulations on a triangular lattice with 972 sites

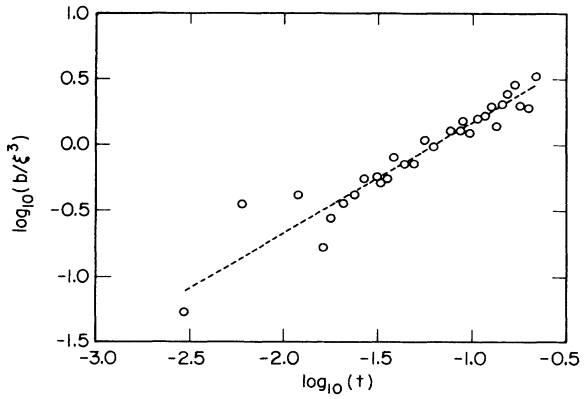

FIG. 12. Log-log plot for the temperature dependence of the threefold anisotropy b/ξ^3 of the $(\sqrt{3}\times\sqrt{3})$ lattice gas above T_c; the fit gives the correction to scaling exponent Δ.

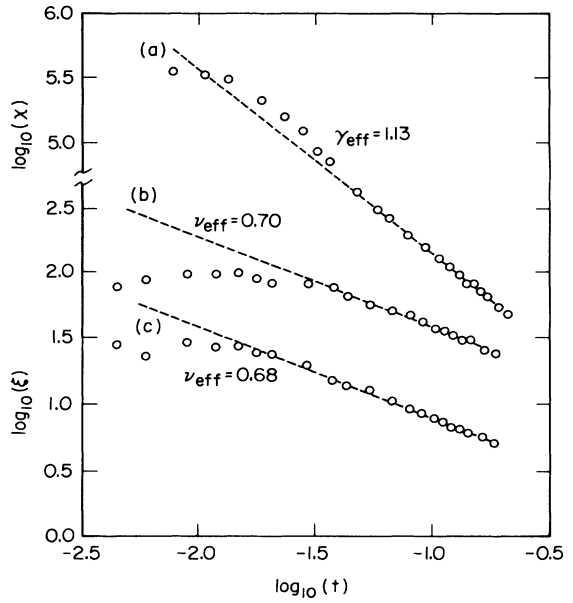

FIG. 13. Log-log plots of (a) χ, (b) ξ derived from cut $\bar{\Sigma}$, and (c) ξ derived from cut T' for the $p(2\times2)$ lattice gas above T_c with $T_c=0.344E_1$.

yield 4.1 ± 0.02 and 43 ± 3 for $0.015<t<0.10$.[40] Including a nonlinear term in the thermal scaling field yields $\beta_{\rm eff}=0.083\pm0.009$, $\nu'_{\rm eff}=0.47\pm0.07$, $\gamma'_{\rm eff}=1.65\pm0.16$, and $T_c^*=0.344\pm0.002E_1$ (see Figs. 14 and 15). The corrections to scaling are expected to be logarithmic. Fitting to the form[42] $t^{2\beta}(1+b[\ln(t)]^{1/8})$ gives $\beta_{\rm eff}=0.078\pm0.020$ [Fig. 14(b)] and $T_c^*=0.343\pm0.002E_1$. Notice there are no significant differences in $\gamma_{\rm eff}$ for cuts $\overline{MK}$ and $\overline{M\Gamma}$ above or below T_c. In contrast to the

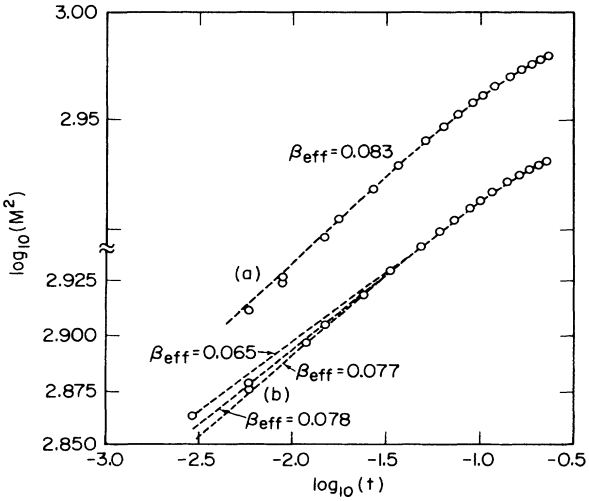

FIG. 14. $\log_{10}(M^2)$ vs $\log_{10}(t)$ for the $p(2\times2)$ lattice gas: (a) $T_c=0.344E_1$; (b) $T_c=0.343E_1$. In (a) the fit assumes a nonlinear term in the scaling field; in (b) the upper fit assumes no corrections, the middle fit assumes $(\log t)^{1/8}$ corrections, and the lower fit assumes a nonlinear scaling field.

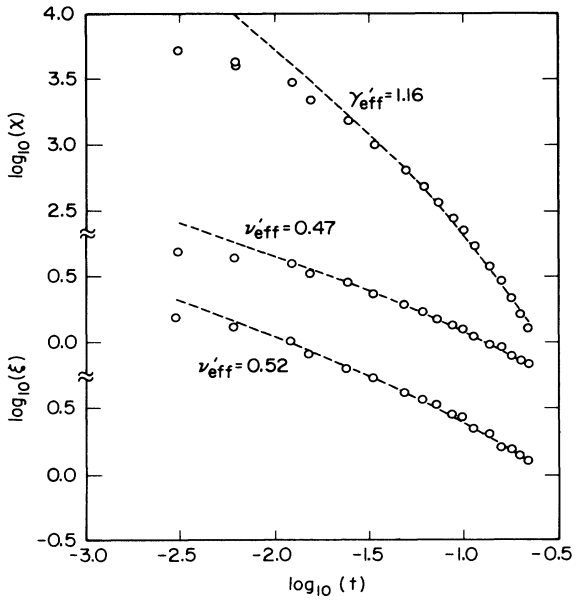

FIG. 15. Log-log plots below $T_c=0.343E_1$ for the $p(2\times2)$ lattice gas: (a) χ; (b) ξ derived from cut $\overline{\Sigma}$; and (c) ξ derived from cut $\overline{T}'$. The fits included a nonlinear thermal scaling field.

$(\sqrt{3}\times\sqrt{3})$ case, where the irrelevant scaling field improved the fits over the one performed with a nonlinear term in the thermal field, here there is no significant difference—which shows the difficulty of determining the source of corrections from such limited data. If we neglect corrections to scaling, we find $\beta_{\text{eff}}=0.066$, similar to the result of Saito[18] for a similar problem.

Figure 16 shows the temperature dependence of the ratio of the correlation lengths in the radial and azimuthal directions. If the scaled structure factor were isotropic, this ratio would approach unity as T approached T_c. From Fig. 16 it is not obvious that it does. Thus there is the possibility that the quadratic gradient term which distinguishes the $p(2\times2)$ Hamiltonian from that of the four-state Potts model [see Eq. (12)] is relevant or sufficiently large to cause different critical behavior. The behavior in Fig. 16 contrasts with the behavior we have observed for the ratio of the correlation lengths in two perpendicular directions of the four-state Potts model on a 972 site triangular lattice: The ratio was 1.0 ± 0.05 for $t<0.10$, showing clearly the irrelevancy of the lattice. Notice the anisotropy in the case of the $p(2\times2)$ is *not* simple lattice anisotropy.[43]

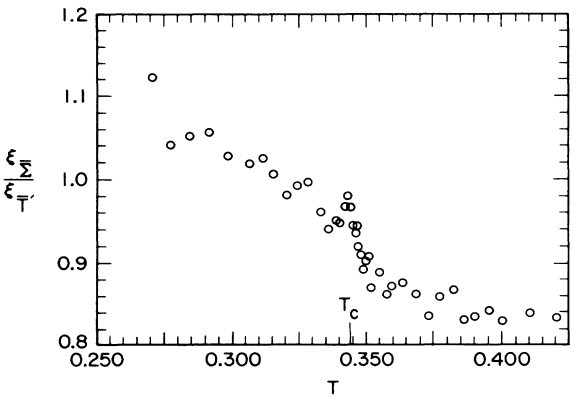

FIG. 16. Temperature dependence of the ratio of the ξ's derived from cuts $\overline{\Sigma}$ and $\overline{T}'$ of the $p(2\times2)$ lattice gas. Note that it does not evidently become unity as $T_c\approx0.344E_1$, indicating there is the possibility that the scaled structure factor is anisotropic and thus not Potts-like.

VI. ROLE OF DEFECTS

In typical experiments on chemisorbed systems the coverage does not change as the temperature is raised because chemisorbed systems are not usually in equilibrium with a gas phase, or any other reservoir of particles, as assumed in the grand canonical ensemble used in our Monte Carlo experiments. Away from high-symmetry points in the phase diagrams, this introduces a fixed concentration of annealed defects, in the form of vacancies, for example. As the concentration of defects (or coverage) is a singular function of T in the grand canonical ensemble away from peaks in phase boundaries (that is when $\partial T_c/\partial\mu$ is nonzero), the critical exponents are Fisher renormalized.[44] Fisher renormalization changes the specific heat exponent α to $-\alpha/(1-\alpha)$, while the exponents β, γ, and ν change by a factor of $1/(1-\alpha)$. To explicitly show this effect we performed constant-coverage Monte Carlo simulations for the $p(2\times2)$ triangular lattice gas at a coverage of 0.21 (816 atoms on our 3888 site lattice). The peak of the phase boundary is between a coverage of 0.25 and 0.26. The result for $S(\overline{M})$ is shown in Fig. 17. Comparison with Fig. 3(c) shows that the transition is now considerably broader. The data, unfortunately, do not allow accurate determination of the effective exponents. They are, however, consistent with β three $[1/(1-2/3)]$ times as large as the values found in the preceding section. More convincing is the data for the energy and specific heat, also shown in Fig. 17. All signs of any divergence are gone. That there is no sign of even a cusp implies that α is less than -1. (The Fisher-renormalized α is -2.) It is

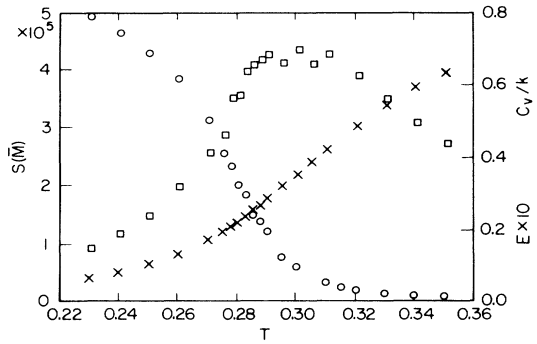

FIG. 17. Temperature dependence of $S(\overline{M})$ (○), the energy (×), and the specific heat (□) for the $p(2\times2)$ lattice gas at a fixed coverage 16% below saturation, illustrating Fisher-renormalized smoothing of the transition.

difficult to distinguish the behavior of Fig. 17 from a first-order transition: as the coverage and $S(\bar{M})$ generally change discontinuously at first-order transitions, crossing the coexistence region would yield a range of temperatures where the energy changes linearly with temperature, similar to the temperature dependence of $S(\bar{M})$ and energy in Fig. 17. Fisher renormalization occurs for any type of annealed defects—weakly bound impurities for example.

Another type of defect one expects to encounter on surfaces is quenched defects, that is random defects which are not in thermal equilibrium with the surface.[45] As these defects will usually favor one locally ordered state over another, they act as random fields,[46] which destroy long-range order in two dimensions.[45] Thus quenched defects act as a finite-size effect: they set a limit, L_D, on the correlation length. To show the effect on the structure factors we performed simulations on the $(\sqrt{3}\times\sqrt{3})$ lattice gas where we had introduced random configurations of quenched vacancies. Figure 18(a) compares the structure factors of the nondefective system with a system with 3% (viz. 117) quenched vacancies 2.7% above T_c. (We averaged results from ten different defect distributions; although this number is not sufficient to obtain good statistics, it is adequate for our qualitative purposes.) At this temperature the correlation length for the nondefective system is much larger than the distance between defects, and thus the structure factor at small $|\mathbf{k}|$ changes dramatically [$S(\bar{K})$ changes by a factor of 3]. At larger $|\mathbf{k}|$ the effect is less, as one would expect: at wavelengths less than the distance between defects the correlation functions are not much affected. This is in accord with the scaling hypothesis.

$$S(\mathbf{k},T,L_D)=t^{-\gamma}X(\xi/L_D,k\xi)\ , \tag{22}$$

that is, when kL_D is large one crosses over to the perfect-system behavior. At temperatures 10% above T_c, when the correlation length is smaller than L_D, we observe that $S(\mathbf{k})$ is not affected as much for 3% defects [Fig. 18(b)], again consistent with the form of Eq. (22). The lesson here is that quenched defects operate as a finite-size effect: To an experimenter they limit the range of T and $\mathbf{k}$ he can study for information about the critical behavior of the perfect infinite system.

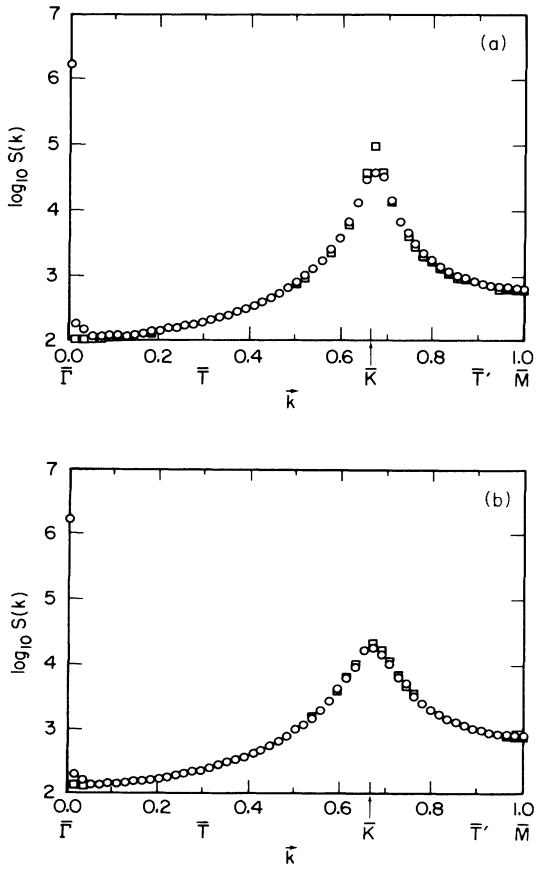

FIG. 18. Log[$S(\mathbf{k})$] for the $(\sqrt{3}\times\sqrt{3})$ lattice gas with 3% quenched vacancies (○), and no defects, (□) at temperatures (a) 2.7% and (b) 10% above the T_c of the perfect system, showing finite-size-like rounding in the immediate vicinity of the transition.

VII. CONCLUSION

Our goal has been to determine the effect of various limitations, especially modest step or defect-free lattice size, on attempts to study critical behavior in two-dimensional systems using diffraction measurements. As shown by Fig. 4, the structure factor, at least above T_c can be expected to scale over a wide range of temperatures and wave vectors. With our "ideal" data, we have explored the issues that arise in analysis and offered guidelines on how best to proceed. Above T_c we find effective susceptibility and correlation-length exponents which are within of order 10% of the expected values. Below T_c, perhaps as a symptom of smaller correlation lengths, we find larger corrections to scaling. We suggest that, as this feature is expected to be universal, it is dangerous (or at least not optimal), for example, to use the order parameter squared to find T_c by maximizing linearity on a log-log plot or to rely solely on the magnetization exponent β for classification.[47]

This paper has investigated two-dimensional critical phenomena from the diffraction viewpoint, implicitly assuming the product of wave vector (or inverse "instrumental range") and correlation length is small. It thus complements our recent work[10] in the opposite limit, in which this product is large and in which one probes criticality from measurements of short-range rather than long-range order. The deduced values of the effective specific heat exponent are of comparable accuracy to the exponents found here. Since it is generally easy to achieve this limit in experiments by degrading instrumental resolution, these sorts of measurements should be included in any investigation to two-dimensional phase transitions.

In all the lattice gases studied, we clearly observed lower symmetry than in the Potts model of the same universality class. These asymmetries arise from low-order gradient terms in the LGW Hamiltonians which are absent in the Potts models. Such terms are neglected in the standard Landau theory identification[14,15] of the

universality class. For the $(\sqrt{3}\times\sqrt{3})$ lattice gas they are clearly irrelevant. For the $p(2\times2)$ system, the seeming relevance or marginality of the gradient correction term, if substantiated, would also contradict conventional Landau classification. We have also seen that the ratio of the susceptibilities above and below T_c has important experimental consequences. Except for the Ising model, there have been no calculations to our knowledge of this universal quantity for two-dimensional systems.

In research parallel to this study, we have also considered the disordering transitions of two other lattice gases. The first is the melting of a (3×1) overlayer on a centered rectangular lattice gas.[48(a)] This transition is evidently continuous from a non-high-symmetry point to an incommensurately disordered phase. Huse and Fisher[7] predict that this transition belongs to a new universality class, and indeed the product of the correlation length and incommensurability *appears* to approach a constant as the transition is approached. The second additional system studied was the melting of a $p(2\times2)$ overlayer on a honeycomb lattice.[48(b)] The melting appears to be first order with the correlation length growing large near the transition.

In summary, we have seen that for lattices with defect-free regions currently under study, one can obtain critical exponents that can—but just barely—be used to distinguish universality classes. Furthermore, in real systems there will be the additional complications of unknown boundary conditions, shapes, and distribution of sizes of defect-free regions. While any physical corroboration, however crude, of theories of two-dimensional criticality is exciting and worthwhile, we argue that experimentalists should strive for significantly better surfaces (and instruments) so that meaningful data an order of magnitude closer to T_c can be measured. Only in this way can information be obtained that will challenge details of current theories.

ACKNOWLEDGMENTS

This work was supported by the U. S. Department of Energy under Grant No. DE-FG05-84ER45071. Computer facilities were supplied by the University of Maryland Computer Science Center. While revising this paper, T.L.E. benefited from the hospitality and support of the Surface Science Division of the National Bureau of Standards.

---

*Also at Department of Physics, Haverford College, Haverford, PA 19041.

[1]For example, L. D. Roelofs and P. J. Estrup, Surface Sci. **125**, 51 (1983); E. Bauer, in *Phase Transitions in Surface Films,* edited by J. G. Dash and J. Ruvalds (Plenum, New York, 1980), p. 267.

[2]For example, P. Kleban, in *Chemistry and Physics of Solid Surfaces,* edited by R. Vanselow and R. Howe (Springer, Berlin, 1984) Vol. V, p. 339.

[3]O. G. Mouritsen, *Computer Studies of Phase Transitions and Critical Phenomena* (Springer, Berlin, 1984).

[4]K. Binder, in *Monte Carlo Methods in Statistical Physics,* edited by K. Binder (Springer, Berlin, 1979), Chap. 1; K. Binder and D. Stauffer, in *Applications of the Monte Carlo Method in Statistical Physics,* edited by K. Binder (Springer, Berlin, 1984), Chap. 1.

[5]M. N. Barber, in *Phase Transitions and Critical Phenomena,* edited by C. Domb and J. L. Lebowitz (Academic, London, 1983), Vol. 8, p. 145.

[6]R. H. Swendsen, in *Phase Transitions: Cargèse, 1980,* edited by M. Levy, J.-C. LeGuillou, and J. Zinn-Justin (Plenum, New York, 1982), p. 395.

[7]D. A. Huse and M. E. Fisher, Phys. Rev. Lett. **49**, 793 (1982); Phys. Rev. B **29**, 239 (1984).

[8]R. L. Park, J. E. Houston, and D. G. Schreiner, Rev. Sci. Instrum. **42**, 60 (1971).

[9]J. M. Cowley, *Diffraction Physics* (North-Holland, Amsterdam, 1981), and references therein.

[10]N. C. Bartelt, T. L. Einstein, and L. D. Roelofs, Phys. Rev. B **32**, 2993 (1985).

[11]L. D. Roelofs, Ph.D. thesis, University of Maryland, 1980 (unpublished).

[12]L. D. Roelofs, A. R. Kortan, T. L. Einstein, and R. L. Park, Phys. Rev. Lett. **46**, 1465 (1981).

[13]N. C. Bartelt, T. L. Einstein, and L. D. Roelofs, Phys. Rev. Lett. **56**, 2881 (1986).

[14]S. Alexander, Phys. Lett. **54A**, 353 (1975); E. Domany, M. Schick, J. S. Walker, and R. B. Griffiths, Phys. Rev. B **18**, 2209 (1978).

[15]M. Schick, Prog. Surf. Sci. **11**, 245 (1981).

[16]W. Kinzel and M. Schick, Phys. Rev. B **23**, 3435 (1981); B. Mihura and D. P. Landau, Phys. Rev. Lett. **38**, 977 (1977); D. P. Landau, Phys. Rev. B **27**, 5604 (1983).

[17]J. Glosli and M. Plischke, Can. J. Phys. **61**, 1515 (1983).

[18]Y. Saito, Phys. Rev. B **24**, 6652 (1981).

[19]Complete high-symmetry cuts took about $\frac{1}{20}$ of the CPU time it took to propagate the lattice; *individual* points in **k** space away from high-symmetry axes required $\frac{1}{40}$ of the propagation time.

[20]M. E. Fisher, Proc. Nobel Symp. **24**, 16 (1974).

[21]C. A. Tracy and B. M. McCoy, Phys. Rev. B **12**, 368 (1975).

[22]P. Kleban, G. Akinci, R. Hentschke, and K. R. Brownstein, J. Phys. A **19**, 437 (1986).

[23]N. C. Bartelt and T. L. Einstein, J. Phys. A **19**, 1429 (1986).

[24]D. A. Huse, Phys. Rev. B **29**, 5031 (1984).

[25]P. W. Schmidt and M. Chandrasekhar, Phys. Rev. B **24**, 2773 (1981).

[26]M. P. M. den Nijs, J. Phys. A **17**, L295 (1984).

[27]D. Friedan, Z. Qiu, and S. Shenker, Phys. Rev. Lett. **52**, 1575 (1984).

[28]A. Aharony and M. E. Fisher, Phys. Rev. B **27**, 4394 (1983).

[29]M. E. Fisher and R. J. Burford, Phys. Rev. **156**, 583 (1967).

[30]T. L. Einstein, in *Chemistry and Physics of Solid Surfaces,* edited by R. Vanselow and R. Howes (Springer, Berlin, 1982), Vol. IV, Chap. 11.

[31]K. Binder, J. Stat. Phys. **24**, 69 (1981).

[32]K. Binder and D. P. Landau, Phys. Rev. Lett. **52**, 318 (1984);

J. Als-Nielsen, in *Phase Transitions and Critical Phenomena,* edited by C. Domb and M. S. Green (Academic, London, 1976), Vol. 5a, Chap. 3. See also M. Fähnle and J. Souletie, J. Phys. C **17**, L469 (1984); Phys. Rev. B **32**, 3328 (1985); A. S. Arrott, *ibid.* **31**, 2851 (1985).

[33]For example, P. R. Bevington, *Data Reduction and Error Analysis for the Physical Sciences* (McGraw-Hill, New York, 1969). We did not carry through this tedious analysis completely for every uncertainty quoted. In particular, the errors quoted for the $P(2\times2)$ are only estimates gained from experience with the $(\sqrt{3}\times\sqrt{3})$.

[34]Our quoted uncertainties are of the same order of magnitude as many of those quoted for experiments (see Ref. 12 for an example). However, they are roughly half an order of magnitude greater than those reported in J. C. Campuzano, M. S. Foster, G. Jennings, R. F. Willis, and W. Unertl, Phys. Rev. Lett. **54** (1985), and J. C. Campuzano, G. Jennings, and R. F. Willis, Surf. Sci. **162**, 484 (1985). One explanation for the difference could be that the data of Campuzano *et al.* has less uncertainty than our Monte Carlo data. Examination of the scatter in their data makes this implausible, however.

[35]F. Y. Wu, Rev. Mod. Phys. **54**, 235 (1982).

[36]We located T_c by finding the temperature where the cumulant of a block distribution function of the order parameter approached a nontrivial "fixed point" as the block size increased, as described in K. Binder, Z. Phys. B **43**, 119 (1981). Because the order parameters in the systems studied here have more than one component, the appropriate cumulants are different from those in Binder's study of the Ising model. For the $(\sqrt{3}\times\sqrt{3})$ lattice gas the cumulant studied was $\langle\,|\,\mathrm{Im}(\psi^3)\,|\,\rangle_L/\langle\,|\,\mathrm{Re}(\psi^3)\,|\,\rangle_L$, where $\psi(\mathbf{r})$ is the complex local order-parameter field.

[37]Different definitions of the correlation length have different universal ratios. For example correlation lengths from $-\lim_{r\to\infty}(1/r)\langle s(0)s(r)\rangle$ have a ratio of 2 for the Ising model.

[38]The ratio squared is Σ_2^+/Σ_2^- of Eq. (2.14) of Ref. 21. See also E. Barouch, B. M. McCoy, and T. T. Wu, Phys. Rev. Lett. **31**, 1409 (1973).

[39]We computed the amplitude ratios by performing a least-squares fit which assumed the Potts model exponents and the T_c obtained in the analysis of χ above T_c.

[40]For the q-state Potts model we defined the structure factor as $S(\mathbf{k})=\langle\,|\,\sum_{\mathbf{r}}\hat{\epsilon}(\mathbf{r})e^{i\mathbf{k}\cdot\mathbf{r}}\,|^2\rangle$, where $\hat{\epsilon}(\mathbf{r})$ points to one of the q symmetric directions of a hypertetrahedron in $q-1$ dimensions.

[41]B. Nienhuis, J. Phys. A **15**, 199 (1982).

[42]J. L. Cardy, M. Nauenberg, and D. J. Scalapino, Phys. Rev. B **22**, 2560 (1980).

[43]In the anisotropic Ising model the scaled structure factor is anisotropic, with the anisotropy technically marginal: A. D. Bruce, J. Phys. C **7**, 2089 (1974).

[44]M. E. Fisher, Phys. Rev. **176**, 257 (1968).

[45]For a recent review, see G. Grinstein, in *Fundamental Problems in Statistical Mechanics,* edited by E. G. D. Cohen (Elsevier, Amsterdam, 1985), Vol. VI, p. 147.

[46]W. Kinzel, Phys. Rev. B **27**, 5819 (1983); L. D. Roelofs, Appl. Surf. Sci. **11/12**, 425 (1982); R. Birgeneau and A. N. Berker, Phys. Rev. B **26**, 3751 (1982).

[47]I. F. Lyuksyutov and A. G. Fedorus, Zh. Eksp. Teor. Fiz. **80**, 2511 (1981) [Sov. Phys.—JETP **53**, 1317 (1981)].

[48]N. C. Bartelt, T. L. Einstein, and L. D. Roelofs, (a) Phys. Rev. B (to be published); (b) (unpublished).